

Investigation of Structural and Optical Properties of CdS, ZnO, ZnS Thin Film for Heterojunction Solar Cell

T. Kamal¹, F. A. Sohaly¹

^{1,2}Department of Electrical and Electronic Engineering, University of Dhaka

Abstract: In this work, CdS, ZnS and ZnO thin films have been deposited by chemical bath deposition technique and dried at 150°C for 30 min. Detail optical and structural characterizations have been done by UV-Vis spectroscopy and X-ray Diffraction analysis to get a comparative study between 3 samples. The XRD analysis has revealed that CdS and ZnO have hexagonal wurtzite crystal structures while ZnS has Zinc blend crystal structure. Lattice parameter and crystallite size were also measured from XRD. From UV spectra it is seen that ZnS and ZnO have transmittance in the range of (85-90) % which was greater than that of CdS. Deposited CdS, ZnS and ZnO reportedly have band gaps of 2.0 eV, 3.63 eV and 3.65 eV respectively. It is proposed that among 3 samples ZnO has more suitable properties as the window layer for thin film solar cell.

Keywords: Buffer layer; Chemical bath deposition; XRD; UV-Vis spectroscopy; Extinction coefficient

I. INTRODUCTION

Owing to superior performance, long term stability, environment cleanliness and high efficiency, thin film/ZnS/ZnO chalcopyrite solar cells have received extensive attention in recent times [1]. Cadmium sulfide (CdS), Zinc sulfide (ZnS) and Zinc oxide (ZnO) are compound semiconductor comprising of group II–VI elements [2 - 5].

Because of direct wide band gap (3.55 eV at room temperature), large exciton binding energy (60meV), and superior conducting properties based on oxygen vacancies, the wurtzite-structured Zinc oxide (ZnO) has become one of the most promising materials having lots of research interest due to their unique structural, electrical, optical and mechanical properties that can be manipulated by changing the dimension [6-7, 10]. One of the main reasons for ZnO popularity among semiconductor materials is their potential applications in nano-devices, as optical materials as well as a buffer layer in solar cell [8-9]. CdS is an intrinsic n-type semiconductor with relatively wide band gap (2.42 eV at room temperature [11-13]. CdS is widely used in a variety of fields, such as light emitting diodes [14], photonic devices [15-17], photoconductive sensors [18] and environmental pollution control [18]. These properties make it a very desirable as the window layer for many heterojunction thin film solar cells. Zinc sulfide (ZnS) is considered to be a significant material in the development of optoelectronic applications, since it is a wide band gap (3.6 eV for cubic ZnS at room temperature) semiconductor [19]. This material has huge potential applications as both bulk and thin film form in various photovoltaic and optoelectronic devices. It is used as key material for solar control coating, optoelectronic devices, electroluminescence devices, sensors and others [20].

Numerous preparation techniques have been stated for thin film deposition i.e. spray pyrolysis, electrode position, solution growth, sol-gel, successive ionic layer of adsorption and reaction (SILAR), vacuum deposition, sputtering, sintering, sublimation, molecular beam epitaxy etc.[21]. In our study we have prepared CdS, ZnO and ZnS thin films by chemical bath deposition method (CBD) to have a comparative study between them using XRD and UV-Vis spectroscopy data.

II. EXPERIMENTAL

CdS, ZnS and ZnO thin film layers were deposited on soda lime glass substrate (1.5 inch X 1 inch) using Chemical Bath Deposition process. For CdS deposition, cadmium chloride and thiourea were used as precursors. Deposition time and temperature were 70 min and 60°C respectively. For ZnS synthesis, zinc chloride and thiourea acted as the precursors with deposition time 30 min and temperature 75°C. Zinc acetate dihydrate was used as precursor for synthesizing ZnO layer with temperature 60°C and deposition time 2h. pH was kept between 8-9 for ZnS, 10-11 for CdS and ZnO. Before each reading pH meter was cleaned to avoid any kind of contamination. Monoethanolamine was used as stabilizer for ZnO and ammonia for CdS and ZnS. Hereafter; samples were dried at 150°C for 30 min to remove the extra moisture and other inorganic substances.

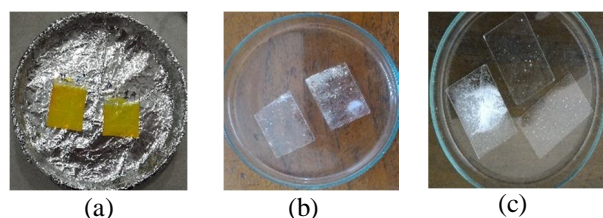


Fig. 1: (a) Deposited CdS films, (b) Deposited ZnS films, (c) Deposited ZnS films

III. RESULTS AND DISCUSSION

A. XRD

X-ray diffraction experiment was carried out using PANalytical X-ray diffractometer (Model: EMPYREAN, PANalytical, Almelo, Netherland) with Cu-K α radiation wavelength of 0.15418 nm, operated at 45 kV and 40 mA. Experiment was carried out at room temperature with the scanning angular range $10^\circ \leq 2\theta \leq 70^\circ$ to get possible fundamental peaks for each sample. Fig. 2 shows crystallite structure and phase purity of synthesized CdS, ZnS and ZnO samples. The peak positions of all samples correspond to CdS, ZnS and ZnO respectively according to the standard JCPDS card. CdS [21] and ZnO are reported to have hexagonal wurtzite crystal structure whereas ZnS is indexed as cubic or zinc-blend structure. Presence of (111) plane confirm this statement. For CdS, other than the fundamental peaks there were peaks of quartz at (112) and (100) plane indicating slight impurity of the samples. ZnO have no other diffraction peaks other than ZnO indicating absence of any impurity phase. ZnS has one peak of SnS at (102) which indicates some of the Sn may have reacted with sulfur and form a crystal of their own. Average crystal size, microstrain, dislocation density and lattice constant were also measured from XRD data using Debye-Scherrer's equation (1) and are given in Table 1.

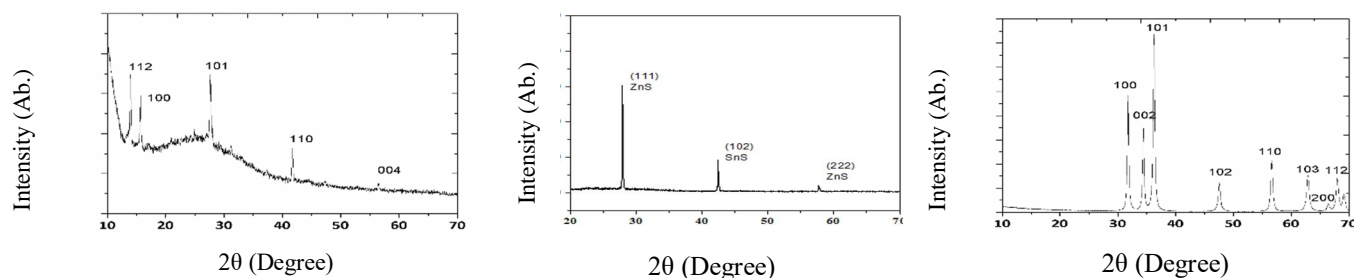
$$D = \frac{0.9\lambda}{\beta_{hkl}\cos\theta} \quad (1)$$

Here β = FWHM of the structural broadening, D = average crystallite size, λ = incident X-ray beam wavelength (1.541 Å) and θ = Bragg's diffraction angle [25]. The strain (ϵ) along the c-axis for the samples was calculated by (2) -

$$\epsilon = \frac{\beta\cos\theta}{4} \quad (2)$$

Dislocation densities for the samples were estimated using WilliamSon-Smallman equation (3)

$$\delta = \frac{1}{D^2} \quad (3)$$



(a) XRD graph for CdS buffer layer

(b) XRD graph for ZnS buffer layer

(c) XRD graph for ZnO buffer layer

Fig. 2: XRD patterns of (a) CdS (b) ZnS (c) ZnO samples deposited by CBD Process for Heterojunction Solar Cell

TABLE I

Average crystal size, microstrain, dislocation density and lattice constant values for CdS, ZnS and ZnO samples.

Sample	2θ value (°)	FWHM (β)	Average Crystal Size, D (nm)	Micro-strain (ε) (10 ⁻³)	Dislocation density (δ) /nm ² (10 ⁻³)	a = b	c
CdS	28.0	0.085	24.12	0.0206	1.7188	4.1502	6.7381
ZnS	27.9	0.073	22.42	0.309	1.9894	5.4247	5.4247
ZnO	36.5	0.299	35.54	1.242	0.7917	3.2447	5.1994

B. Transmittance and Absorption Calculation:

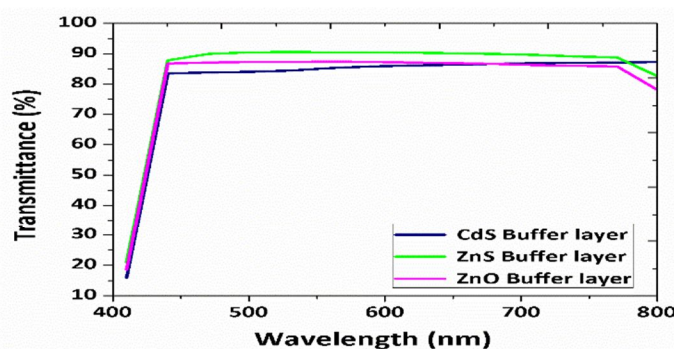
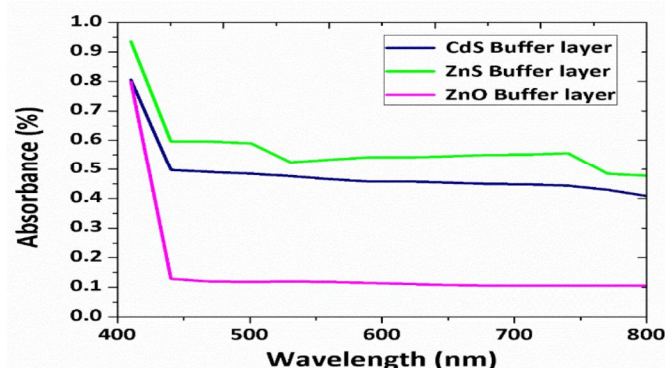
Experiments for obtaining optical transmission spectra (T%) were performed at room temperature using UV-Vis spectroscopy in the range of 400-800 nm as displayed in Fig.3. Transmittance curves as a function of wavelength for the nanostructure CdS, ZnS and ZnO thin films are shown. The films of ZnS and ZnO are highly transparent and have transmittance in the range of 85%-90% which is relatively higher than that of CdS. ZnS has higher transmittance than ZnO and CdS. As one can see from Fig. 3 that transmittance rises rapidly above 80% for wavelength above 450nm. In addition, a slight shift of optical absorption edge to higher wavelength values is observed. Below 450nm there is a sharp fall in the percentage transmittance of the films, an indication of a strong increase in absorption. This is attributed to rapid change in the optical absorption coefficient and is an indication that some states have been Created in the region between the conduction and valence band [22]. This can also be attributed to the increase in fundamental absorption as photon striking increases with increase in carrier concentration [20]. The absorbance values of all the films are calculated from transmittance and reflectance data using the expression

$$T+R+A=I, \quad (4)$$

$$\text{So that } A = I - [T+R] \quad (5)$$

Fig. 4 shows that CdS, ZnS and ZnO films have good absorption at short wavelength region (below 450nm), the absorption decreased with increasing wavelength of solar radiation. For ZnS film, the graph shows slight non-linearity in the decreasing region, this could have happened for the non-uniformity and roughness of film surface.

Fig. 3: Transmittance as a function of wavelength for the



nanostructure CdS, ZnS and ZnO thin film. Fig. 4: Absorbance as a function of wavelength for the nanostructure CdS, ZnS and ZnO thin film.

C. Extinction Coefficient Calculation

Extinction coefficients of the 3 samples were measured in the range of photon wavelength from 400 nm to 800 nm. The extinction coefficient, k is the imaginary part of the complex index of refraction which also relates to the light absorption [21]. Here, extinction co-efficient has been calculated for CdS, ZnS and ZnO samples deposited on soda lime glass substrate using absorption co-efficient values of the thin films. Fig 5(a) shows the extinction coefficient response with respect to wavelength values and Fig. 5(b) gives the extinction coefficient response with respect to the photon energy values. Equation (6) is used to calculate the extinction co-efficient values from absorption co-efficient and wavelength values.

$$k = \frac{\alpha \lambda}{4\pi} \quad (6)$$

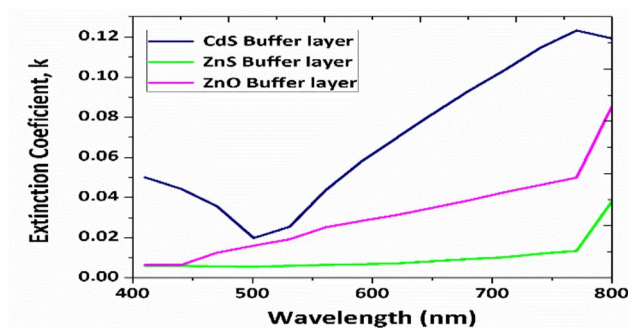


Fig. 5(a): Extinction coefficient of the samples vs. wavelength (nm)

Here, k = extinction co-efficient, α = absorption co-efficient and λ = incident wavelength from UV-vis NIR. It can be seen from (6) that extinction co-efficient is proportional to the absorption co-efficient and wavelength. Fig. 5(a) shows that the extinction coefficient increases according to the increase of wavelength (nm). Fig. 5(b) displays exactly the opposite that, the extinction coefficient gradually decreases according to the increase of photon energy (eV). It is known that the extinction coefficient describes the attenuation of light in a medium [23]. That means the higher value of k represents the greater attenuation of light in a thin film. Here, ZnS has lower attenuation for having lower extinction co-efficient values and CdS has higher attenuation for having higher extinction co-efficient values. ZnO has an intermediate value between CdS and ZnS. As for the window layer of a solar cell less attenuation of light is expected [23], ZnS and ZnO will be good options.

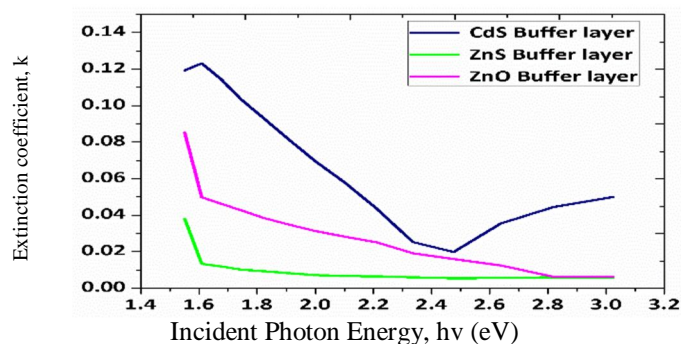


Fig. 5(b): Extinction coefficient of the samples vs. photon energy (eV).

D. Refractive Index Calculation

Refractive index of 3 different samples has been discussed and analyzed in the photon wavelength from 400 nm to 800 nm and in the photon energy from 1.6 eV to 3 eV. The refractive index is an important property for optical characterization which can be used in many optical applications [25]. Here, refractive index has been calculated for CdS, ZnS and ZnO thin films using the reflectance (%) values of these thin films. Fig. 6(a) and Fig. 6(b) show refractive index response with respect to wavelength (nm) and photon energy (eV) respectively. Refractive index (η) calculation from reflectance (R) values is given by (7) –

$$\eta = \frac{1 + \sqrt{R}}{1 - \sqrt{R}} \quad (7)$$

The refractive index values of different samples are different. CdS shows a slight gradual increase with wavelength and slight gradual decrease with photon energy. For ZnS, refractive index first decrease a bit in 430-450 nm range then gradually increases. This value decreases in case of photon energy for ZnS but starts to increase after 2.8 eV photon energy. This decrement in case of wavelength may be caused due to some defects formed in the deposited films [24]. Because of this defect light will get absorbed here [15]. Refractive index for ZnO refractive index gradually decreases with wavelength but in 750-770 nm regions it started to increase again. Opposite case is seen for photon energy. All three samples have different values of refractive index in same region of wavelength and photon energy.

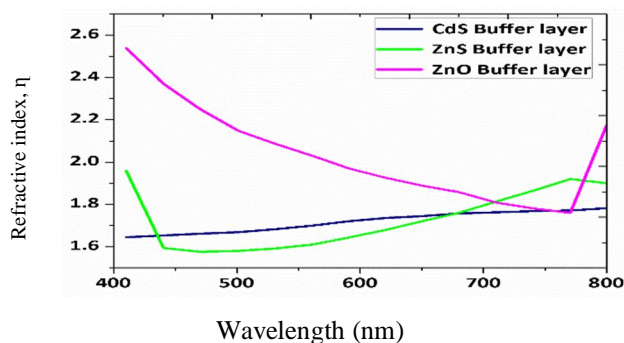


Fig. 6(a): Refractive index of the samples vs. wavelength (nm).

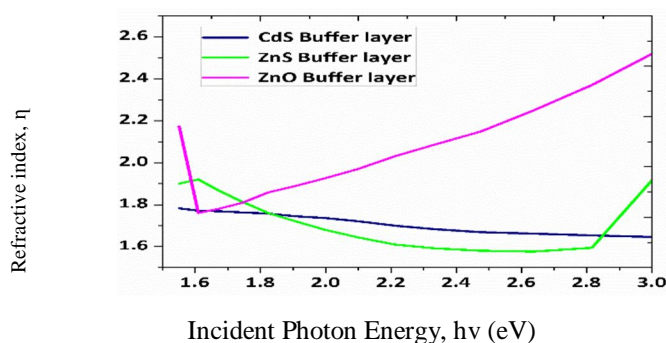


Fig. 6(b): Refractive index of the samples vs. incident photon energy (eV).

E. Bandgap Calculation

In semiconductors, the relation connecting the absorption coefficient α , the incident photon energy ($h\nu$) and optical band gap E_g takes the form of (8) -

$$(ah\nu) = k (h\nu - E_g)^n \quad (8)$$

where ν = frequency of the incident photon, h = Planck's constant ($\sim 6.63 \times 10^{-34}$), k = a constant which is different for different transitions and it is related to the effective masses (of electron and hole) associated with the bands [23] and n = the number which characterizes the optical processes, $n = 1/2$ for a direct allowed transition, 2 for the indirect allowed transition, $3/2$ for a forbidden direct transition and 3 for a forbidden in direct transition [24]. Band gap energy (E_g) is derived from the mathematical treatment of the data obtained from the absorbance vs. wavelength spectrum for direct band gap CdS, ZnS and ZnO using Tauc's relationship [24].

$$(ah\nu)^2 = A (h\nu - E_g) \quad (9)$$

Absorption coefficient (α) is evaluated from the relation $A = 2.303\alpha t$ and using the measured values of thicknesses (t), which were 136.94 nm for CdS, 100 nm for ZnO and 230 nm for ZnS deposited films.

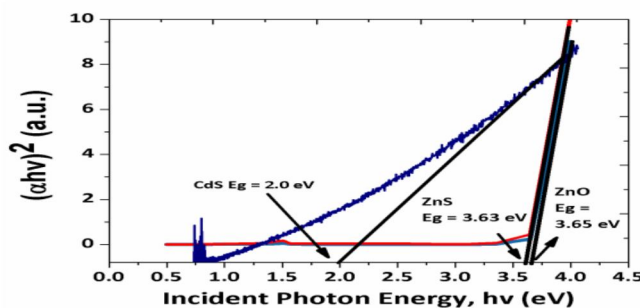


Fig 7: Band gap values determined by Tauc plot of CdS, ZnS and ZnO samples.

Fig. 7 shows the plot of $(\alpha h\nu)^2$ as a function of photon energy ($h\nu$). Extrapolation of the line to the base line, where the value of $(\alpha h\nu)^2$ is zero, gives band gap (E_g) [24]. The sharp absorption edge corresponding to the band gap confirms the good quality of the films. It is observed that the direct band gap for CdS, ZnS and ZnO thin films are 2.0 eV, 3.63eV, 3.65eV respectively. ZnS and ZnO have higher band gap value than CdS which is very much effective and expected for buffer layer in solar cell. As it is known that buffer layer admits photo generated carrier to absorber layer with minimal absorption loss and recombination loss and transport the photo generated carrier with minimal resistive loss [22]. For this optical throughput it needs a window layer with bandgap as high as possible and layer as thin as possible [23]. Among these 3 samples ZnS and ZnO satisfy both of these conditions.

IV. CONCLUSION

CdS, ZnS and ZnO buffer layer for hetero junction solar cell have been successfully deposited by chemical bath deposition technique and dried at 150°C for 30 min. CBD is chosen as the deposition technique for its low cost, vacuum free and environment friendly set up. XRD measurement revealed that ZnS has zinc blend structure while CdS and ZnO have hexagonal wurtzite structure with slight impurity. To increase the efficiency of solar cell buffer layer needs to be highly transmittive. UV-Vis spectroscopy showed that ZnO has moderately high transmitting capability than CdS but slightly less than ZnS. ZnO also reported to have lower attenuation value and higher bandgap of 3.65 eV. Considering all these findings from this work it is proposed that ZnO will be more suitable as buffer layer than CdS and ZnS.

V. ACKNOWLEDGMENT

For this work authors are grateful to Atomic Energy Center, Dhaka, Department of Glass and Ceramics, Bangladesh University of Engineering and Technology, Dhaka, and Bangladesh Council of Scientific and Industrial Research, Dhaka, Bangladesh.

REFERENCES

- [1] Pino D'Amico, ArrigoCalzolari, Alice Ruini&AlessandraCatellani Scientific Reports, 2017,volume 7, Article number: 16805.
- [2] K. Benyahia, A. Benhaya and M. S. Aida; 2015 Chinese Institute of Electronics Journal of Semiconductors, Volume 36, Number 10
- [3] Anwar H. Ali, Sarah A. Jassem, World Scientific News, EISSN 2392-2192.
- [4] AixiangWei, JunLiu, MixueZhuang, YuZhao, Materials Science in Semiconductor Processing, Volume 16, Issue 6, December 2013, Pages 1478-1484
- [5] AyanMukherjeea, ParthaMitraa Materials Research, DOI: <http://dx.doi.org/10.1590/1980-5373-MR-2016-0628>
- [6] AlexanderAxelevitch, BorisApter, Microelectronic Engineering Volume 170, 25 February 2017, Pages 39-4
- [7] K.P. Shinde, R.C. Pawar, B.B. Sinha, H.S. Kim, S.S. Oh, K. C. Chung, J. Alloys Compd, 08.030 2014.
- [8] Park, Sang Yong; Park, JeongEun Eom, Taewoo Park, Jeong Hun; Bweupe, Jackson; Lim, Donggun;Journal of Nanoscience and Nanotechnology, Volume 18, Number 9, September 2018, pp. 6294-6299(6)
- [9] W. Widiyastuti, Iva Maula, TantularNurtono, FadlilatulTaufany,SitiMachmudah, SugengWinardi, Camellia Panatarani, "Preparation of zinc oxide/silica nanocomposite particles via consecutive sol gel and flame-assisted spray-drying methods", Chem. Eng. J. 2014, 254 252-258).
- [10] Jiazhen Sheng, Hyun-Jun Jeong, Ki-Lim Han, TaeHyunHong&JinSeong Park, Journal of Information Display;Volume 18, 2017 - Issue 4
- [11] Khaled Ben Messaoud, Guy Brammertz, Marie Buffière, SouhaibOueslati, HossamElAnzeery, Marc Meuri, MosbahAmlouk and JefPoortmans, Published 3 November 2017, Materials Research Express, Volume 4, Number 11
- [12] A. Hasnat, J.Podder, Journal of Bangladesh Academy of Science Vol. 37, No. 1, 33-41, (2013).
- [13] C. Schwartz, D. Nordlund, T. Weng, D. Sokaras, L. Mansfield, A. S. Krishnapriyan, K. Ramanathan, K. E. Hurst, D. Prendergast, S. T. Christensen, Solar energy materials and solar cells, Vol. 149, p. 275-283 (May 2016).
- [14] P. A. Nwofeand P. E. Agbo, Effect of Deposition Time on the Optical Properties of Cadmium Sulphide Thin Films, Int. J. Thin. Fil. Sci. Tec. 4, No. 2, 63-67 (2015).
- [15] R. Demir, F. Gode, Structural, optical and electrical properties of nanocrystalline CdS thin films grown by CBD, Chalcogenide Letters Vol. 12, No. 2, p. 43 – 50 (February 2015).
- [16] Rongrong Chen, Jiandong Fan, Chong Liu, Xing Zhang, YanjiaoShenYaohua Mai, Scientific Research Published: 13 October 2016
- [17] M A Islam, S. Hossain, N. Amin, M. M. Aliyu, Y. Sulaiman and K. Sopian, Advanced Materials Research Vols. 622-623 pp 1194-1198(2013).
- [18] Ezenwa I. A., Effect of Film Thickness on the Transmittance of Chemical Bath Fabricated CdS Thin Film, Advances in Applied Science Research, 3 (5):2826-2829 (2012).
- [19] Daniela E. Ortíz-Ramosa, Luis A. González, Rafael Ramirez-Bonb, "p-Type transparent Cu doped ZnS thin films by the chemical bath deposition method", Materials Letters 124 267–270 (2014).
- [20] J. N. Alexander, S. Higashiya, D.CaskeyJr, H. Efsthadiadis, P.Haldar, Deposition and characterization of cadmium sulfide (CdS) by chemical bath deposition using an alternative chemistry cadmium precursor, Solar Energy Materials & Solar Cells 125 47–53 (2014).
- [21] Kumar V, Saroja M, Saroja M, Venkatachalam M and Shankar S, International Journal of Recent Scientific Research ISSN: 0976-3031 Volume: 6(11) November -2015.
- [22] T. Kamal, S. Parvez, K. M. Khabir, R. Matin, T. Hossain, H. Sarwar, M. S. Bashar, M. J. Rashid, South Asian Journal of Research in Engineering Science and Technology, Vol. 02 Issue. 03, pp 610-617 (2017).
- [23] TaherGhrib, Muneera Abdullah Al-Messiere,andAmalLafi Al-Otaibi Journal of Nanomaterials Volume 2014
- [24] Feroza.Mir;Results in Physics Volume 4, 2014, Pages 103-104